AD-A142 199 MULTIPLE SCATTERING EFFECTS IN EXAFS (EXTENDED X-RAY 1/1
ABSORPTION FINE STRU..(U) WASHINGTON STATE UNIV PULLMAN
DEPT OF PHYSICS V A BIEBESHEIMER ET AL. 29 MAY 84 TR-5
UNCLASSIFIED N00014-82-K-0530 F/G 7/4 NL

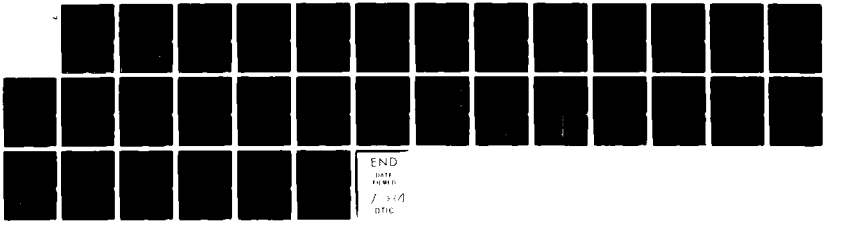

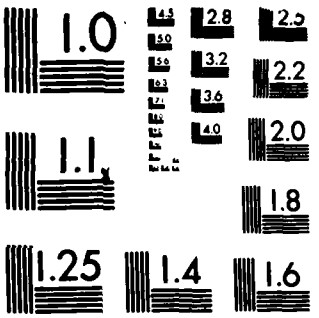

MICROCOPY RESOLUTION TEST CHART
NATIONAL BUREAU OF STANDARDS-1963-A

OFFICE OF NAVAL RESEARCH

Contract N00014-82-K-0530

Task No. NR 359-823

TECHNICAL REPORT NO. 5

Multiple Scattering Effects in EXAFS: Comparison between Theory and Experiment for Pt Metal

by

V. A. Biebesheimer, E. C. Marques, D. R. Sandstrom,

F. W. Lytle, and R. B. Greegor

Prepared for Publication

in the

Journal of Chemical Physics

Washington State University
Department of Physics
Pullman, WA 99164-2814

May 29, 1984

SECURITY CLASSIFICATION OF THIS PAGE (When Data Entered)

REPORT DOCUMENTATION PAGE

READ INSTRUCTIONS BEFORE COMPLETING FORM

1. REPORT NUMBER: Technical Report No. 5	2. GOVT ACCESSION NO.: AD-A142 199
3. RECIPIENT'S CATALOG NUMBER:	
4. TITLE (and Subtitle): Multiple Scattering Effects in EXAFS: Comparison Between Theory and Experiment for Pt Metal	5. TYPE OF REPORT & PERIOD COVERED: Technical Report
	6. PERFORMING ORG. REPORT NUMBER:
7. AUTHOR(s): V. A. Biebesheimer, E. C. Marques, D. R. Sandstrom, F. W. Lytle, and R. B. Greegor	8. CONTRACT OR GRANT NUMBER(s): N00014-82-K-0530
9. PERFORMING ORGANIZATION NAME AND ADDRESS: Department of Physics, Washington State University, Pullman, WA 99164-2814	10. PROGRAM ELEMENT, PROJECT, TASK AREA & WORK UNIT NUMBERS:
11. CONTROLLING OFFICE NAME AND ADDRESS: Leader, Chemistry Division, Office of Naval Research, 800 North Quincy Street, Arlington, Virginia 22217	12. REPORT DATE: May 23, 1984
	13. NUMBER OF PAGES: 31
14. MONITORING AGENCY NAME & ADDRESS(if different from Controlling Office): Office of Naval Research Resident Representative, University of Washington, District Building, Room 422, 1107 Northeast 45th Street, Seattle, Washington 98195	15. SECURITY CLASS. (of this report): Unclassified
	15a. DECLASSIFICATION/DOWNGRADING SCHEDULE:

16. DISTRIBUTION STATEMENT (of this Report)

This document has been approved for public release and sale; its distribution is unlimited.

17. DISTRIBUTION STATEMENT (of the abstract entered in Block 20, if different from Report)

18. SUPPLEMENTARY NOTES

19. KEY WORDS (Continue on reverse side if necessary and identify by block number)

EXAFS, XANES, Multiple scattering, Platinum

20. ABSTRACT (Continue on reverse side if necessary and identify by block number)

EXAFS model functions have been calculated for the L_{III}-edge in Pt metal taking into account all single, double, and triple scattering contributions. Comparison to experimental data shows that multiple scattering effects are important in Pt only at radial distances corresponding to fourth shell nearest neighbors.

DD FORM 1 JAN 73 1473

SECURITY CLASSIFICATION OF THIS PAGE (When Data Entered)

Multiple scattering effects in EXAFS: comparison between theory and experiment for Pt metal

V. A. Biebesheimer, E. C. Marques*, and D. R. Sandstrom

Department of Physics, Washington State University,

Pullman, Washington 99164-2814

F. W. Lytle and R. B. Greegor

The Boeing Company, Seattle, Washington 98124

Extended x-ray absorption fine structure (EXAFS) model functions have been calculated for the L_{III} edge in Pt metal. All single, double and triple scattering contributions were taken into account, using a recently developed multiple scattering formalism. Theoretical values for the scattering amplitude, phase, and Debye-Waller factor and the "universal curve" for the electron mean free path have been used. Comparison to experimental data gives an estimate of the limitations in the current formalism, and shows that multiple scattering effects are important in Pt only at radial distances corresponding to fourth shell nearest neighbors.

PACS Numbers: 78.70.Dm, 61.55.Fe, 34.80.Bm

I. INTRODUCTION

Extended x-ray-absorption fine-structure (EXAFS) measurements have been used in the extraction of structural information in a variety of materials.[1] The single-scattering formula[2]

$$\chi(k) = \frac{|f(\pi,k)|}{kr^2} e^{-2r/\lambda} e^{-2k^2\sigma^2} \sin[2kr + \phi(\pi,k)] \qquad (1)$$

is commonly used to extract information about coordination number, radial distribution, and other relevant parameters. Analysis often involves Fourier-filtering; i. e. the Fourier-transformation of data, filtering out a specific range in the radial distribution and inverse transform of this range. The region commonly used for the inverse transform usually corresponds to the first or second shell of neighbors, since multiple scattering of the electron emitted from the x-ray-absorbing atom is expected at higher radial distances. To use all the data, and to estimate the accuracy of the single scattering equation, it is important to know the effects of multiple scattering. This is specially true in the case of metal structures, since one of the major applications of EXAFS-studies is to small metal clusters in supported catalysts. Recent work has been reported on three-atom molecules in which multiple scattering effects were used for bond-angle determinations.[3,4,5] Multiple scattering effects due to the shadowing effect on the fourth nearest neighbors by the second neighbors in metals with fcc structure have been recognized.[6] A detailed analysis of these effects has not been carried out, partly because theories on multiple scattering effects were not complete.

The present paper examines the importance of multiple scattering and gives an estimate of the accuracy of theoretical calculations. All double scattering contributions to EXAFS are calculated for Pt metal using the

multiple scattering formalism introducted by Lee and Pendry,[6] and later developed by Teo[3] and by Boland et al.[7] Also, all triple scattering contributions are determined where the total scattering path length does not exceed that of fourth shell single scattering. Comparison of the calculated EXAFS function with the measured L_{III} edge of Pt metal gives an estimate of the photoelectron energy range over which EXAFS theories are applicable. Good agreement is found at energies higher than 50 eV above absorption threshold, which shows the limitation of the theories used.

We used unpublished angle dependent phase and amplitude functions calculated by Teo[8] using the programs described previously.[3,9] Published values of these quantities are given only to $k > 4$ because approximations made in their derivation are expected to cause progressively greater inaccuracy at low energies. We used Teo's calculated values down to $k=0.94$ Å^{-1} and extrapolated to $k=0$ Å^{-1} in order to test the multiple scattering theory and calculated quantities over the full range of k. As expected, the calculated EXAFS function becomes less accurate at low energies.

II. THEORY

The multiple scattering expressions for the EXAFS given by Teo[6] and Boland et al.[7] differ only by the presence of a geometrical factor in the double scattering term. We adopt the form that includes it,[7] which, in the case of a polycrystalline sample, is given by:

$$\chi(k) = -\sum_{n=i,j}\Big\{\frac{|f_n(\pi,k)|}{kr_n^2}\sin[2kr_n + 2\delta_\ell(k) + \phi_n(\pi,k)]$$

$$+\frac{2\hat{r}_j\hat{r}_i}{kr_ir_jr_{ij}}|f_i(\beta,k)||f_j(\alpha,k)|\sin[k(r_i+r_j+r_{ij}) + 2\delta_\ell(k) + \phi_i(\beta,k) + \phi_j(\alpha,k)] \quad (2)$$

$$+\frac{|f_i(\pi,k)||f_i(\alpha,k)|^2}{kr_j^2r_{ij}^2}\sin[2k(r_j+r_{ij}) + 2\delta_\ell(k) + \phi_i(\pi,k) + 2\phi_j(\alpha,k)]\Big\}$$

where the symbols have the usual meanings: $k=[2m(E-E_0)/\hbar^2]^{1/2}$ is the photoelectron wave vector; $|f(\alpha,k)|$ the scattering amplitude; $\phi(\alpha,k)$ the scattering phase shift, and δ_ℓ the phase shift due to the central atom potential. The first term is the usual single scattering expression, whereas the second term corresponds to consecutive scattering by atoms i and j, and vice versa. The third term is the result of photoelectron scattering from atom j to atom i, and back to atom j again. To account for inelastic losses of electrons we multiply each scattering path by $\exp(r/\lambda)$, where λ is the electron mean free path and r the total electron path length. A further correction due to thermal vibrations is the inclusion of the Debye-Waller factor $\exp(-2k^2\sigma^2)$, with the mean squared displacement σ^2 dependent on the specific scattering path.

The scattering amplitude and phase functions used in the equation above, and shown in Figs. 1 and 2 were those calculated by Teo[8] at twenty different k-values between 0.9449 Å^{-1} and 15.1178 Å^{-1}, for scattering angles between 0° to 180°, in 5° steps. These values were manually replotted and interpolated on a 78 point grid.

The Pt L_{III} edge central atom phase shift $\delta_{\ell=2}(k)$ values were those calculated by Teo and Lee[9], extended to low k-values by inclusion of unpublished calculations.[8] Although these calculations are based on certain assumptions, excellent agreement has been found with experimentally extracted phase shift data.[10]

For the electron mean free path λ the value of 10 Å was tried at the beginning of this work as a rough estimate. However, much better agreement with experimental data was achieved by using the universal curve[11] for λ, which was used in a tabular form with linear interpolation between points in the range 0.9449 Å^{-1} - 15.1178 Å^{-1} (Table I). It should be noted that this

approach is not consistent with the derivation of the Debye-Waller factor, where a k-independent mean free path is assumed.[12] Most of the variation in λ is at low energies (below 50 eV) where we might expect some disagreement with experimental data.

Our previous study[10] shows that anharmonic disorder effects in Pt are negligible at 100 K and calculations based on the Debye approximation are in excellent agreement with experimentally determined disorder. The Debye-Waller factor was calculated in this approximation, where the mean square displacement (MSD) is given by[13,14,15]

$$\sigma_\infty^2 = \frac{3\hbar}{M\omega_D}\left[\frac{1}{4} + \left(\frac{T}{\theta_D}\right)^2 \int_0^{\theta_D/T} \frac{x}{e^x - 1}\, dx\right] \qquad (3)$$

Since EXAFS is only sensitive to relative displacements, the mean square relative displacement (MSRD) is given by

$$\sigma^2 = 2\,\sigma_\infty^2(1-\gamma) \qquad (4)$$

with the correlation factor γ calculated by:

$$\gamma = \frac{1}{\sigma_\infty^2}\frac{3\hbar}{M\omega_D}\left[\frac{1-\cos(q_D \cdot r)}{2q_D^2 r^2} + \frac{T}{q_D\, r\, \theta_D}\int_0^{\theta_D/T} \frac{\sin\left(q_D\, r\, \frac{T}{\theta_D}\, x\right)}{e^x - 1}\, dx\right] \qquad (5)$$

where the symbols have the following meaning: θ_D=Debye temperature, $\omega_D = k\,\theta_D/\hbar$ Debye frequency and $q_D=(6\pi n/v)^{1/3}$ the Debye wavenumber. Since the correlation is dependent on the radius, the MSRD is also dependent on the scattering path. The parameters used are θ_D=240 K[16], $n/v=6.62\times10^{-28}$ m^{-3},[15] M=195 amu with a corresponding q_D=1.577 Å^{-1}. The calculated results are given in Table II.

In Table III all the parameters needed for calculating the EXAFS equation are shown. Each scattering path is listed separately and is labeled in accordance with the nomenclature used by Lee and Pendry.[6] 1-2-1 indicates a path which goes from the origin to atom j, which is a first shell distance, to first shell atom i, where the distance between j and i is that corresponding to a second shell, and back to the origin. Similarly, 2-1-3 indicates a path from the origin to second shell atom j and then to third shell atom i which is in the first shell of atom j. All the considered triple scattering paths are 1-1-1-1 paths, so they are labeled Ma to Mg, dependent on the scattering path. For each scattering path, Table III gives the scattering angle, the total distance traveled (corrected for thermal expansion at 100 K), and the angle between r_i and r_j. Since there is more than one atom in the different shells, each scattering path has to be multiplied by the number N of different scattering sequences available to the photoelectron. In the case of single scattering, this is just the number of nearest neighbors in the respective shell, whereas in multiple scattering cases many more equivalent scattering paths are possible. Also included in the table (but not in the final calculation) is single scattering by atoms in the fourth shell and the double scattering 1-4-1 and 1-1-4 paths. All these possibilities are nonphysical, since the second shell atoms shadow the fourth shell atoms. For the fourth shell atoms, the operative scattering paths are the 1-1-1-1 paths.

III. CALCULATIONS

The contribution of all the different multiple scattering paths are shown in Fig. 3. The solid line corresponds to the Ma path, multiplied by 0.6 (see Section IV), and is clearly the strongest multiple scattering contribution. Even by adding up the calculated functions from all double

scattering paths, the Ma contribution is still dominant (Fig. 4). The reason for the small amplitude of most of the double and triple scattering paths is the $1/r^2$ dependence of the EXAFS, and also the low values of the backscattering amplitude at high scattering angles. Because the scattering amplitude peaks in the forward direction, a significant contribution from the Ma and Md paths to the EXAFS is expected. All the other triple scattering contributions are orders of magnitude weaker and can be neglected. The Md to Mg paths are only approximations, since the central atom is involved twice, the second time as an ion (ionized when the photon was absorbed), so that the scattering potential and with it the scattering amplitude and phase is expected to be different compared to the non-ionized case. To account for this circumstance, we allow, in modeling the data, the energy threshold E_0 to be different for each scattering path.

IV. RESULTS

The calculated EXAFS functions were compared to experimental data at the Pt L_{III} edge. The complication which arises from the fact that the initial p-state can go to a final state of s or d symmetry is of only minor concern, because it has been shown from theoretical calculations[9] that transitions to the d final states are generally favored by a factor of 50 over the s final states, so that we can use the above equations with the ℓ=2 central atom phase shift. The experimental EXAFS oscillations were isolated by using a cubic spline technique containing three sections. The data were then normalized to the L_{III} component of the smooth absorption background by using the x-ray absorption coefficient parameterization given by McMaster.[17]

The limits of the single scattering approximation can be seen by Fourier-filtering the data in r-space and comparing it with the corresponding model function. Figure 5 shows the filtered spectra (k^1 weighting), where the

allowed inverse transform range was successively increased from the radial distance corresponding to the first shell to all the first four shells. There are no multiple scattering effects expected in the radial range up to the third shell (5 Å), except some negligible contributions from the 1-1-1, 1-2-1 and 2-1-1 paths (Table III), and a comparison of the data with the summed single scattering contribution from the first three shells shows excellent agreement (Fig. 5 A-C). When the fourth shell is included in the filtering process, the single scattering approximation is not appropriate and the corresponding single scattering calculation does not model all the features in the data (Fig. 5 D).

The energy threshold was determined by adjusting E_0 until the Fourier-filtered first shell EXAFS gave agreement in the phase with the calculated first shell model function. The E_0 value is 6 eV above the inflection point. In adding up all the contributions from multiple scattering paths, E_0 was shifted to -12 eV for the Ma and Md paths. To get reasonable agreement with experimental data the EXAFS function corresponding to the Ma path had to be multiplied by 0.6, indicating that the forward scattering amplitude is not as strong as the calculated amplitude functions, which also have the greatest inaccuracy in the forward scattering case. All the other contributions were directly added without any further weighting. Figure 6 shows a comparison of the experimental data to the calculated single scattering contribution and to the sum of all the different scattering paths.

To model the whole Pt L_{III} absorption edge, the calculated EXAFS was superimposed on an edge function.[18] The EXAFS spectra with the added edge is broadened by first convolving it with a Lorentzian broadening function whose width is the sum of the inverse lifetimes of the core hole and the excited electron, and then further convolution with a Gaussian broadening function

whose width accounts for the instrumental resolution (2 eV). A resonance at -2.8 eV with a width of 6 eV gives the best agreement to the Pt white line, together with a Lorentzian broadening of the edge by a width of 4 eV (Fig. 7). Together with the appropriately broadened EXAFS oscillations the normalized model function compared to the experimental data is shown in Fig. 8. There is good agreement above 50 eV and at the edge, but disagreement between 0-50 eV.

V. DISCUSSION

The derivation of the multiple scattering formula of Eq. 2 assumed that the photoelectron was at sufficiently high energy (approximately three times the plasma frequency; > 70 eV in Pt) so that the attractive potential of the central atom nucleus became negligible. This may explain in part the disagreement at low photoelectron energy, where the central atom potential strongly affects the excited electron. The theoretical phase and amplitude functions are also in question at low energies. The mean free path increases very rapidly at low energy, as does the Debye-Waller factor. Therefore all the contributions from different scattering paths have very large amplitudes near the edge and, due to the 2kr term in the phase, oscillate very rapidly, which results in large changes in the model function from only very small (0.1 eV) changes in threshold energy for certain scattering paths.

At higher energy it was possible to model all the features of the EXAFS spectra. Each small feature could be identified although not always precisely correct in position and amplitude. The three atom scattering path Ma was the most important multiple scattering effect and was clearly recognizable in the EXAFS spectra. This may be of special importance for small metallic clusters (in supported metal catalysts, for example), where the clusters may be so small or so shaped as to give different multiple scattering contributions than the bulk metal. By modeling different structures and sizes

and then comparing them to the experimental data it should be possible to extract structural information directly from the unfiltered oscillations. Figure 6 shows that there are some features in the data which are not present in the calculated spectra with the correct amplitude. This is an indication that even with the multiple scattering approximation used here with its attendant theoretical parameters there are still small but significant differences from experimental data.

VI. CONCLUSION

The effects of multiple scattering in Pt metal are only important in the fourth shell region. Multiple scattering contributions corresponding to second and third shell neighbor distances are very weak and can be neglected. At total scattering distances corresponding to the fourth shell, the major contribution to the EXAFS comes from the forward scattering by the second nearest neighbor and backscattering by the fourth shell. This component was clearly identifiable in the experimental data. Generally good agreement with EXAFS data ($E > 50$ eV) was obtained by using the multiple scattering formalism of Eq. 2 and the theoretical angle dependent phase shifts and scattering amplitudes of Teo.[3,8]

ACKNOWLEDGMENTS

This work was supported in part by the National Science Foundation under grant Nos. DMR-8013706 and CHE-8219605 and by the Office of Naval Research. The work reported herein was performed at SSRL which is supported by the Department of Energy, Office of Basic Energy Sciences; the National Science Foundation, Division of Materials Research; and the National Institutes of Health, Biotechnology Resource Program, Division of Research Resources.

REFERENCES

*Present address: Monsanto Company, 800 N. Lindbergh, St. Louis, Missouri 63166.

[1]P. A. Lee, P. H. Citrin, P. Eisenberger, and B. M. Kincaid, Rev. Mod. Phys. 33, 769 (1981).

[2]D. R. Sandstrom and F. W. Lytle, Ann. Rev. Phys. Chem. 30, 215 (1979), Eq. 1.

[3]B. K. Teo, J. Am. Chem. Soc. 103, 3990 (1981).

[4]M. S. Co, W. A. Hendrickson, K. O. Hodgson, and S. Doniach, J. Am. Chem. Soc. 105, 1144 (1983).

[5]N. Alberding and E. D. Crozier, Phys. Rev. B 27, 3374 (1983).

[6]P. A. Lee and J. B. Pendry, Phys. Rev. B 11, 2795 (1975).

[7]J. J. Boland, S. E. Crane, and J. D. Baldeschwieler, J. Chem. Phys. 77, 142 (1982).

[8]We thank Dr. Boon Teo, Bell Laboratories, for making the angle dependent functions for Pt available to us.

[9]B. K. Teo and P. A. Lee, J. Am. Chem. Soc. 101, 2815 (1979).

[10]E. C. Marques, D. R. Sandstrom, F. W. Lytle, and R. B. Greegor, J. Chem. Phys. 77, 1027 (1982).

[11]G. A. Somorjai, Chemistry in Two Dimensions: Surfaces, (Cornell University Press, London, 1981), pp. 41.

[12]G. Bunker, Nucl. Instrum. & Methods 207, 437 (1983).

[13]G. Beni, P. M. Platzman, Phys. Rev. B 14, 1514 (1976).

[14]W. Boehmer and P. Rabe, J. Phys. C: Solid State Phys. 12, 2465 (1979).

[15]P. Rabe, DESY Report No. F41, 1981 (unpublished).

[16]C. Kittel, Introduction to Solid State Physics, 5th Ed. (Wiley, New York, 1976).

[17]W. H. McMaster, N. K. Del Grande, J. H. Mallet, and J. H. Hubbell, Compilation of X-ray Cross Sections, National Bur ·u of Standards Report No. UCRL-SO174, Sec. 11, Rev. 1 (1969).

[18]J. A. Horsley, J. Chem. Phys. 76, 1451 (1982)

TABLE I. Electron Mean Free Path

$k(\mathring{A}^{-1})$	λ ($\mathring{A}$)
0.9449	100.
1.8897	11.69
2.8346	6.11
3.7795	5.15
4.2519	5.21
4.7243	5.47
5.1967	5.80
5.6692	6.10
6.1416	6.49
6.6140	6.95
7.0865	7.35
7.5589	7.71
8.5038	8.66
9.4486	9.38
10.3935	10.28
11.3384	11.10
12.2832	11.69
13.2281	12.56
14.1729	13.28
15.1178	14.05

TABLE II. Disorder Calculation Results for Pt Metal at 100 K

r(Å)	$(q_D r)$	σ_∞^2	γ	σ^2
2.773	4.372	1.490	0.3373	1.975
3.922	6.184	1.490	0.1891	2.417
4.805	7.576	1.490	0.1731	2.465
5.546	8.745	1.490	0.1680	2.480

σ^2 and σ_∞^2 in $(10^{-3}Å^2)$

TABLE III. Multiple Scattering Parameter for Pt.

A. Single Scattering

Shell	r_{total} [a]	σ^2 [b]	N
1.	5.538	1.97	12
2.	7.832	2.42	6
3.	9.595	2.46	24
4.	11.076	2.48	12

B. Double Scattering

Scattering Path	r_{total} [a]	σ^2 [b]	N	Scattering Angle		θ [c]
1-1-1	8.307	3.9	48	120	120	60
1-2-1	9.454	3.9	24	135	135	90
1-1-2	9.454	3.9	48	90	135	45
1-3-1	10.335	3.9	48	150	150	120
1-1-3	10.335	3.9	96	60	150	30
1-4-1	11.076	3.9	12	180	180	180
1-1-4	11.076	3.9	24	0	180	0
1-2-3	11.482	3.9	48	90	145	55
2-1-3	11.482	3.9	48	90	125	35
2-3-1	11.482	3.9	48	145	55	90

C. Triple Scattering

Scattering Path	r_{total} [a]	σ^2 [b]	N	Scattering Angle			θ [c]
Ma	11.076	4.455	12	0	180	0	0
Mb	11.076	4.455	24	90	180	90	0
Mc	11.076	4.455	48	120	180	120	0
Md	11.076	4.455	12	180	0	180	180
Me	11.076	4.455	12	180	180	180	0
Mf	11.076	4.455	24	180	120	180	120
Mg	11.076	4.455	24	180	60	180	60

[a] r_{total} in (Å)

[b] σ^2 in (10^{-3}Å^2)

[c] θ, the central angle, is defined to be the angle between radius vectors from the central atom to the two neighboring atoms in the three-atom problem (cf. Ref. 7).

Captions for Figures

FIG. 1. The scattering amplitude $F(\alpha,k)$ for different scattering angles: 0°(□), 60°(△), 90°(○), 120°(○), 150°(◇), and 180°(▽).

FIG. 2. The scattering phase $\phi(\alpha,k)$ for different scattering angles: 0°(□), 60°(△), 90°(○), 120°(○), 150°(◇), and 180°(▽).

FIG. 3. Calculated EXAFS spectra for different scattering paths: solid line corresponds to Ma path, the dashed lines correspond to the different double scattering paths.

FIG. 4. Calculated EXAFS spectra: single scattering contributions (solid line), double scattering contributions (short dashed line), and the triple scattering contributions (long dashed line).

FIG. 5. Comparison of Fourier-filtered experimental data (solid line) with calculated single scattering, EXAFS spectra (also Fourier-filtered) (dashed line). The radial distance in the filtering corresponds to (A) first, (B) second, (C) third, and (D) fourth shell.

FIG. 6. Comparison of experimental EXAFS spectrum (solid lines) to (A) calculated single scattering involving the first three shells, (dashed line) and (B) sum of single, double and triple scattering contributions, including fourth shell (dashed line).

FIG. 7. Experimental Pt L_{III} absorption edge (solid line) together with the fit (short dashed line) to the sum of the Lorentzian resonance (medium dashed line) and step functions (long dashed line).

FIG. 8. Experimental PT L_{III} absorption edge (solid line) together with the calculated spectra (dashed line).

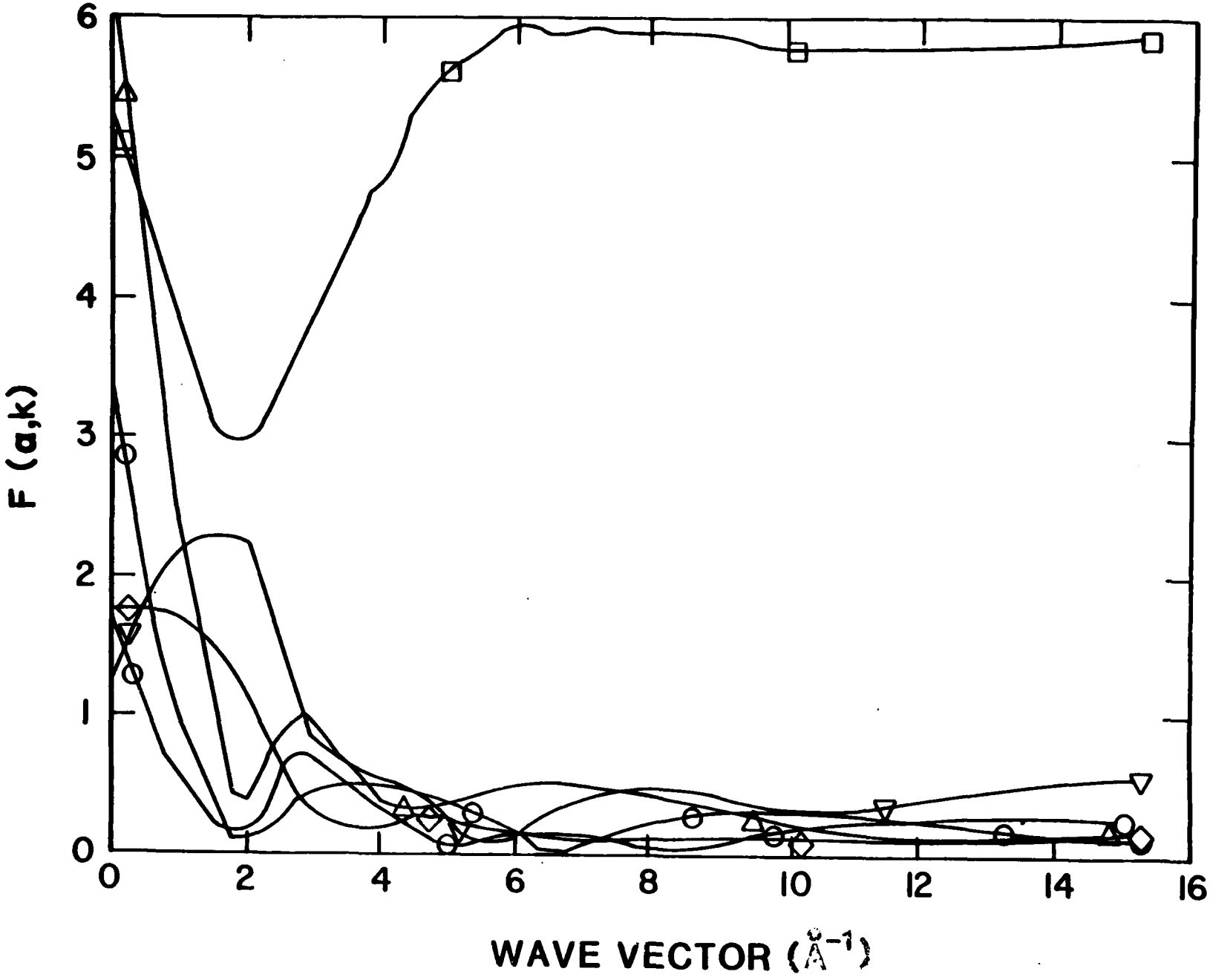
F (a,k)
WAVE VECTOR (Å^{-1})
0
1
2
3
4
5
6
0
2
4
6
8
10
12
14
16

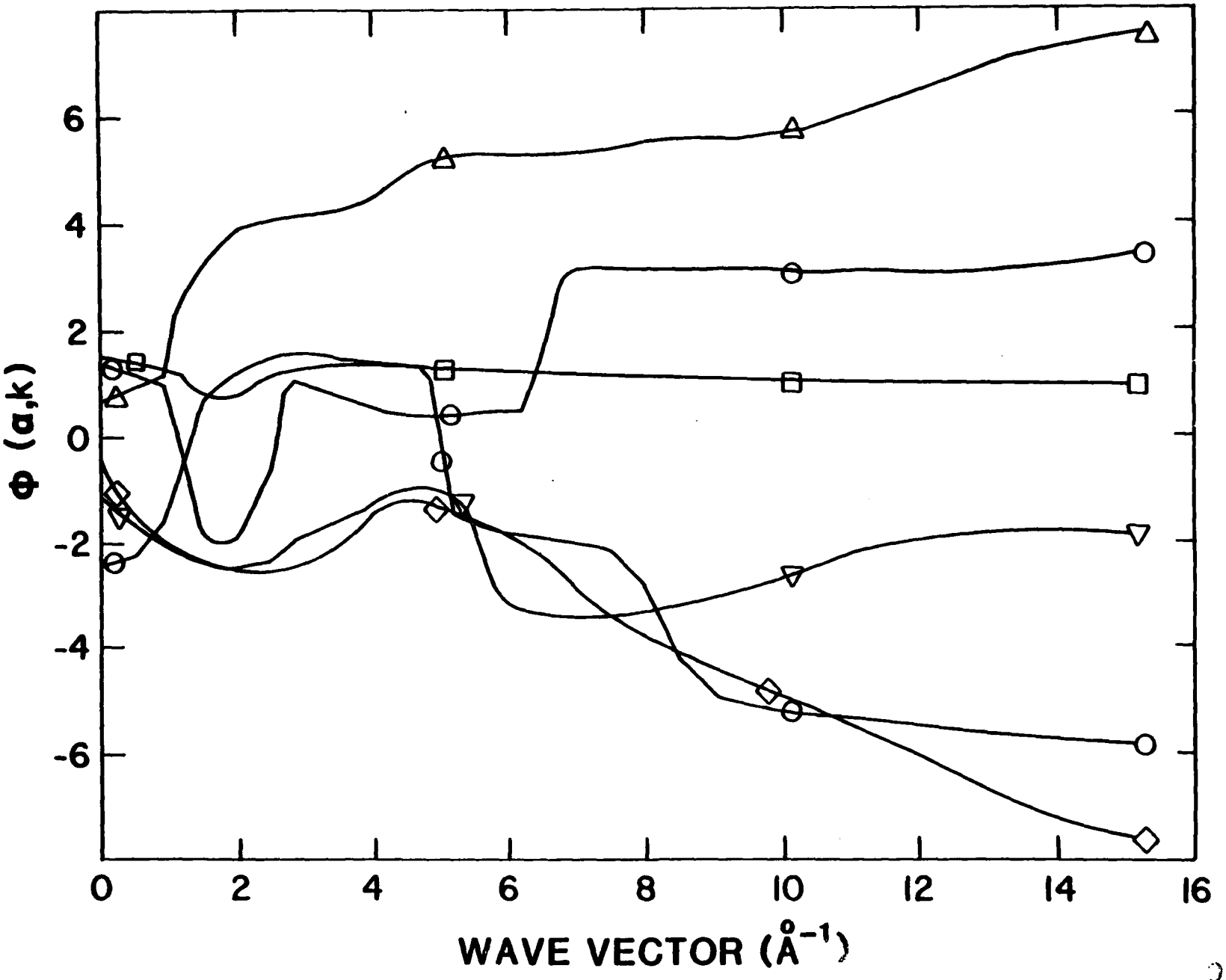
6
4
2
0
-2
-4
-6
Φ (a,k)
0
2
4
6
8
10
12
14
16
WAVE VECTOR (Å^{-1})

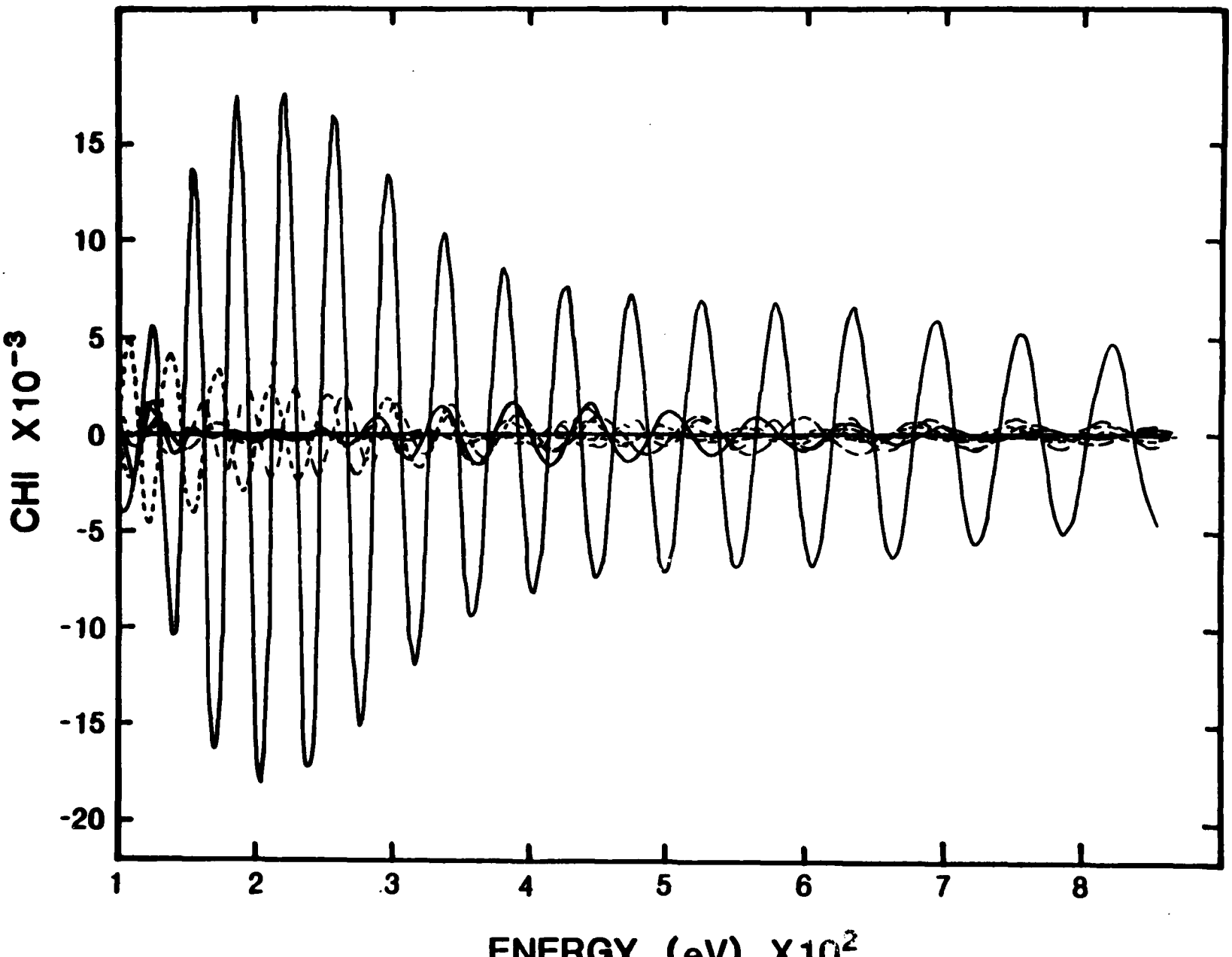
15
10
5
0
-5
-10
-15
-20
CHI X10^{-3}
1
2
3
4
5
6
7
8
ENERGY (eV) X10^2

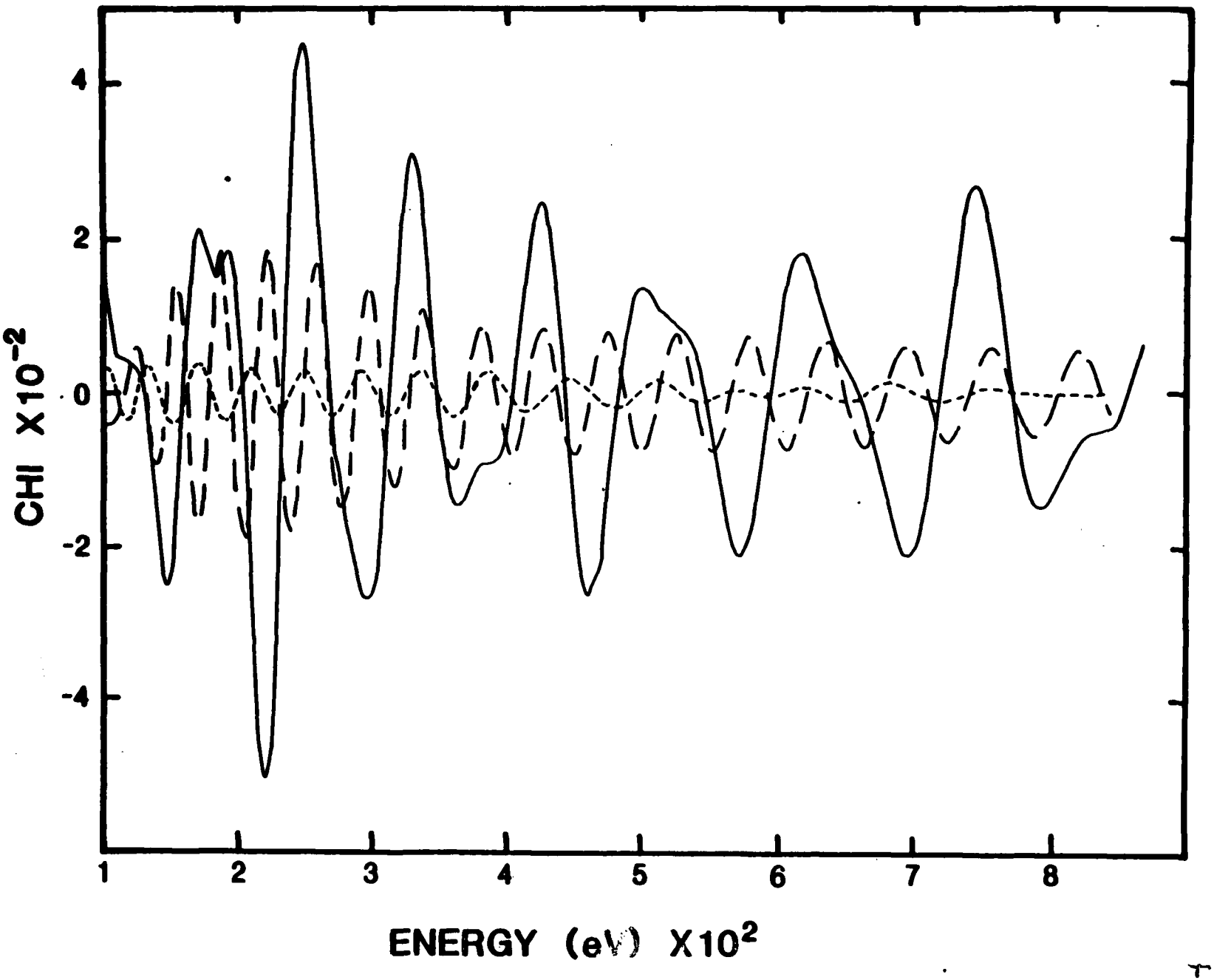
4
2
0
-2
-4
CHI X10^{-2}
1
2
3
4
5
6
7
8
ENERGY (eV) X10^2

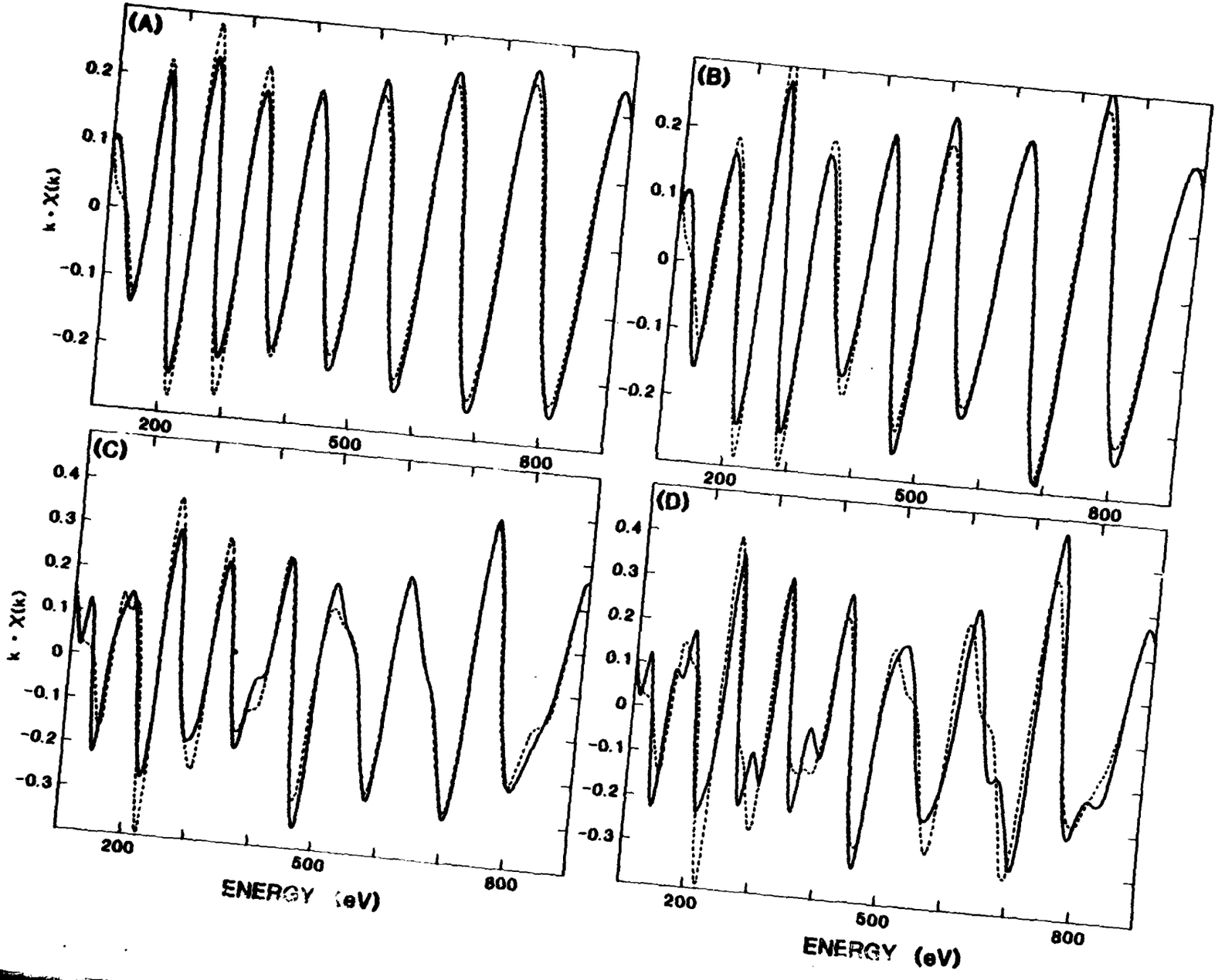
(A)
(B)
(C)
(D)
k · χ(k)
ENERGY (eV)
200
500
800

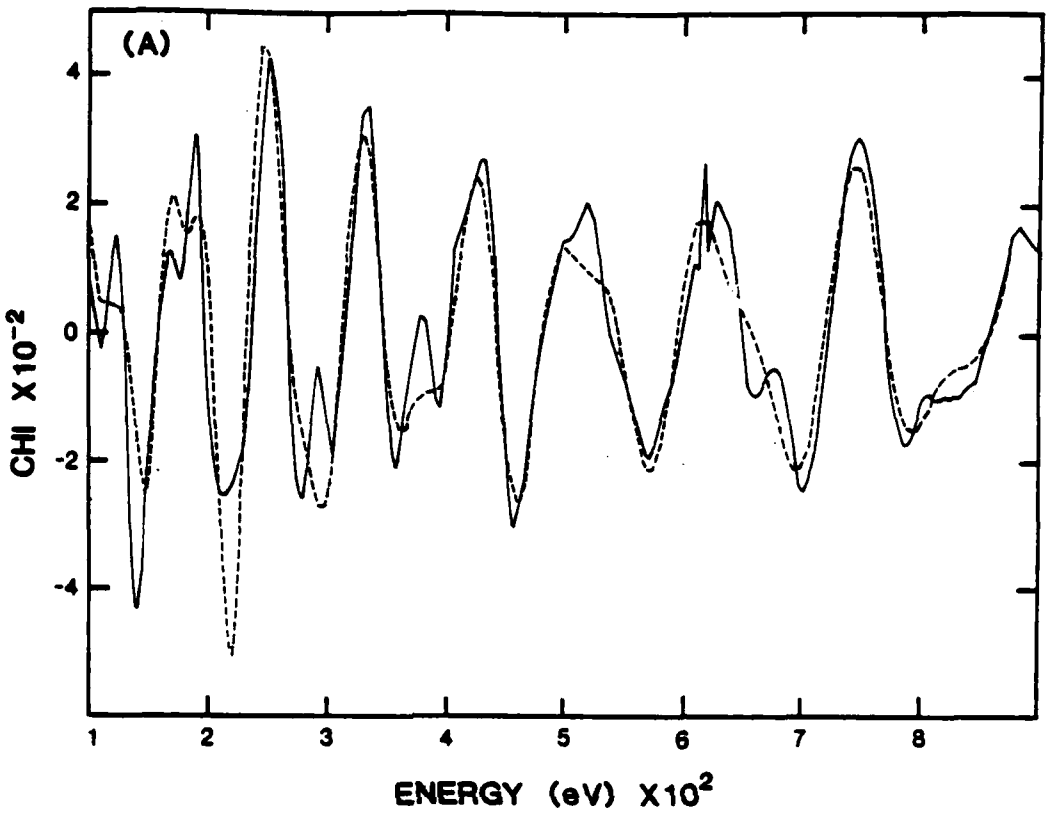
(A)
CHI X10^{-2}
4
2
0
-2
-4
1
2
3
4
5
6
7
8
ENERGY (eV) X10^2

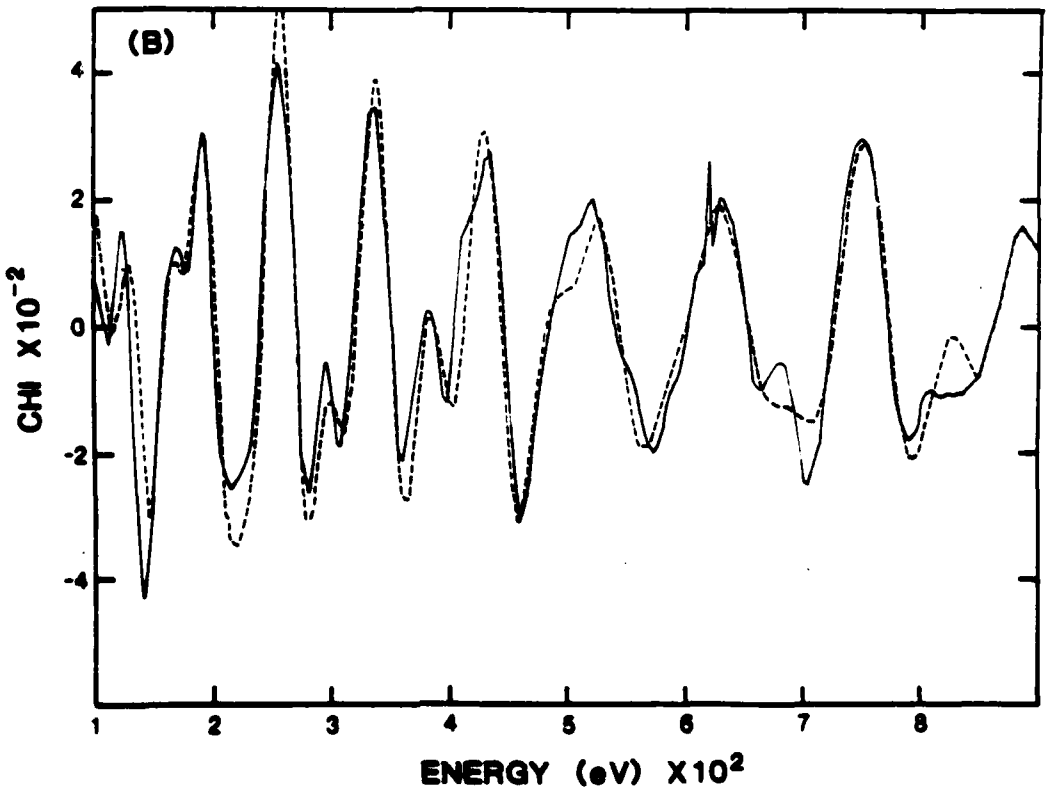
(B)
CHI X10^{-2}
4
2
0
-2
-4
1
2
3
4
5
6
7
8
ENERGY (eV) X10^2

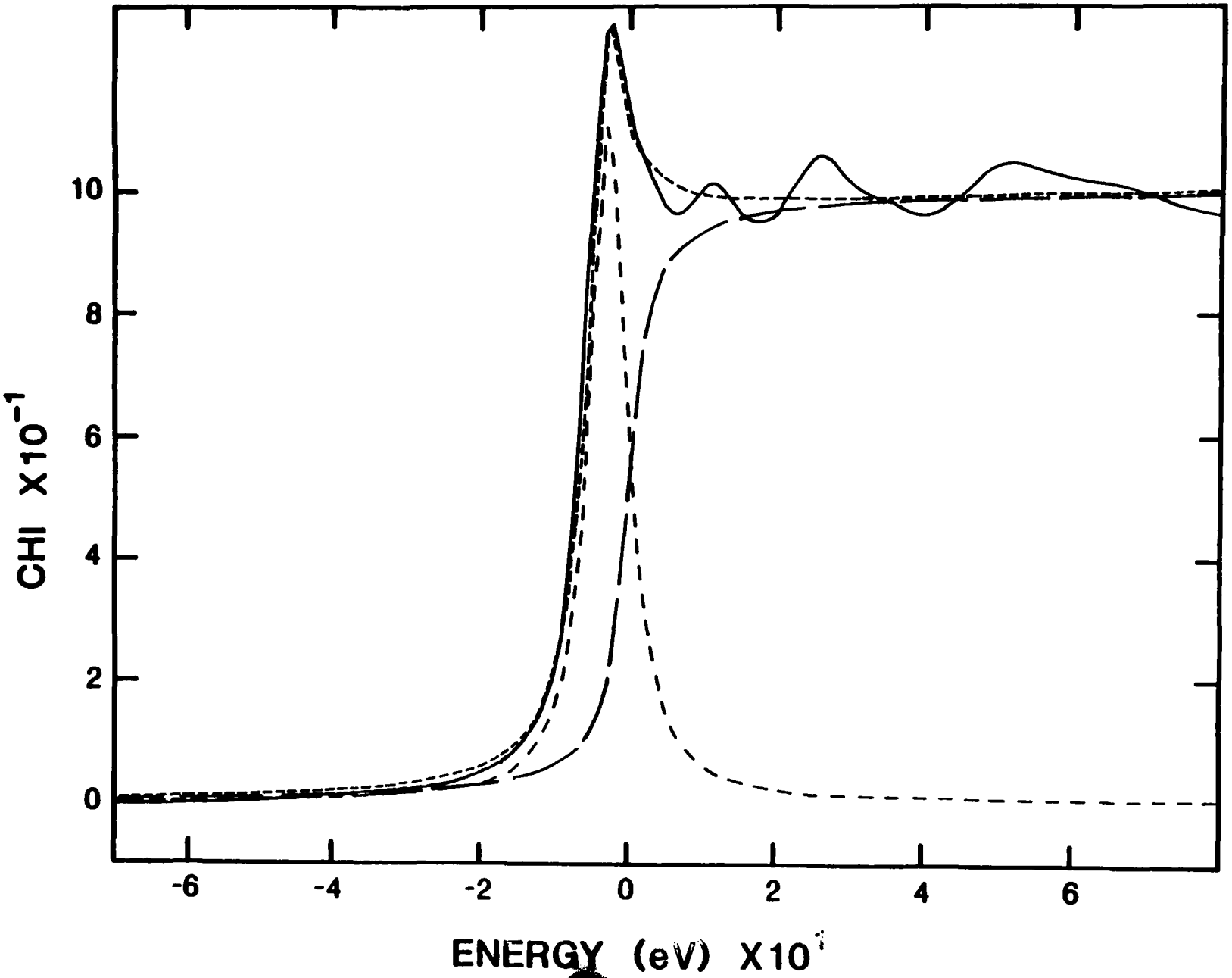
10
8
6
4
2
0
CHI X10^{-1}
-6
-4
-2
0
2
4
6
ENERGY (eV) X10^{1}

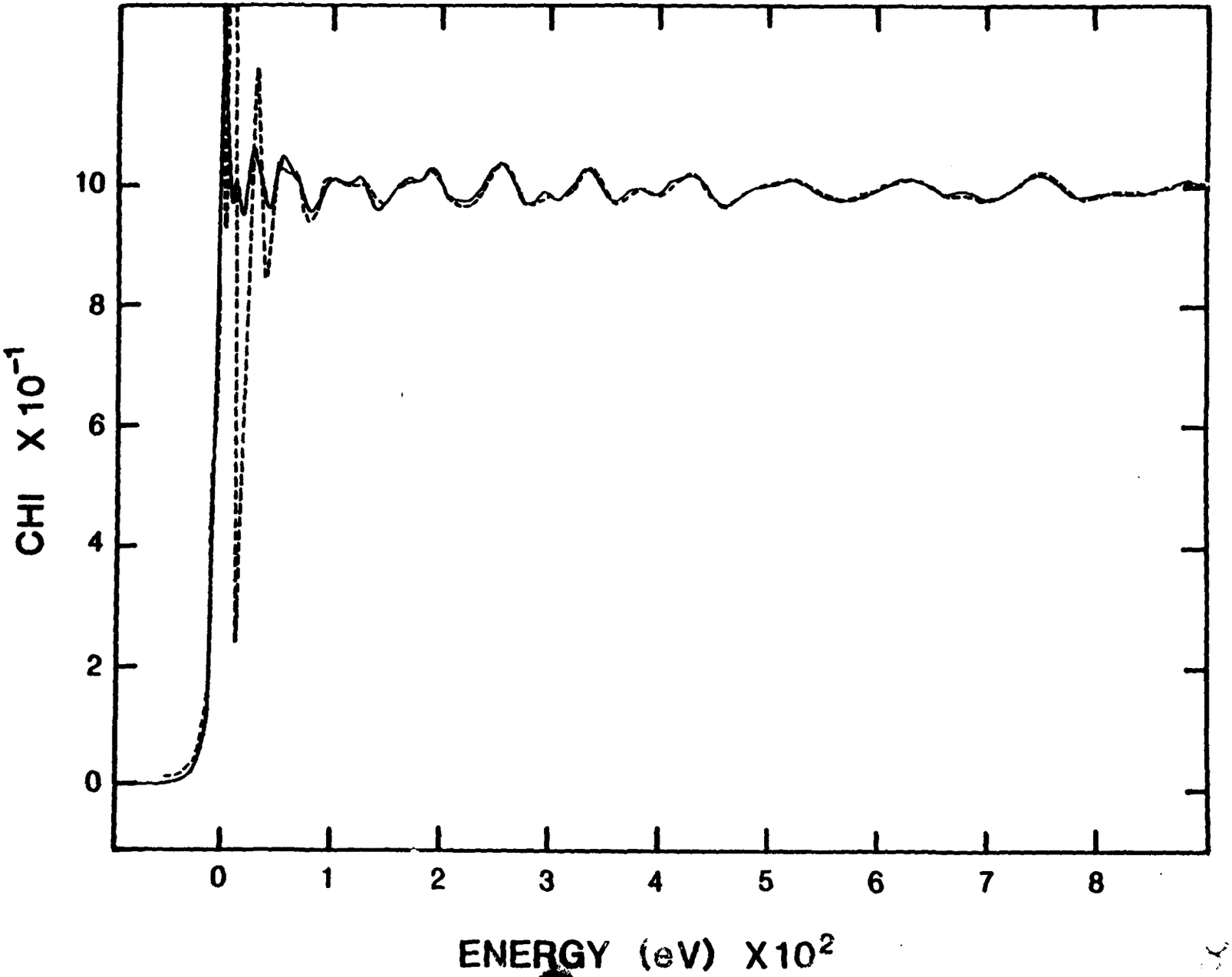
CHI X 10⁻¹
10
8
6
4
2
0
0
1
2
3
4
5
6
7
8
ENERGY (eV) X10²

DL/413/83/01
GEN/413-2

TECHNICAL REPORT DISTRIBUTION LIST, GEN

	No. Copies
Office of Naval Research Attn: Code 413 800 N. Quincy Street Arlington, Virginia 22217	2
ONR Pasadena Detachment Attn: Dr. R. J. Marcus 1030 East Green Street Pasadena, California 91106	1
Commander, Naval Air Systems Command Attn: Code 310C (H. Rosenwasser) Washington, D.C. 20360	1
Naval Civil Engineering Laboratory Attn: Dr. R. W. Drisko Port Hueneme, California 93401	1
Superintendent Chemistry Division, Code 6100 Naval Research Laboratory Washington, D.C. 20375	1
Defense Technical Information Center Building 5, Cameron Station Alexandria, Virginia 22314	12
DTNSRDC Attn: Dr. G. Bosmajian Applied Chemistry Division Annapolis, Maryland 21401	1
Naval Ocean Systems Center Attn: Dr. S. Yamamoto Marine Sciences Division San Diego, California 91232	1
Naval Ocean Systems Center Attn: Technical Library San Diego, California 92152	1
Naval Weapons Center Attn: Dr. A. B. Amster Chemistry Division China Lake, California 93555	1
Scientific Advisor Commandant of the Marine Corps Code RD-1 Washington, D.C. 20380	1
Dean William Tolles Naval Postgraduate School Monterey, California 93940	1
U.S. Army Research Office Attn: CRD-AA-IP P.O. Box 12211 Research Triangle Park, NC 27709	1
Mr. Vincent Schaper DTNSRDC Code 2830 Annapolis, Maryland 21402	1
Mr. John Boyle Materials Branch Naval Ship Engineering Center Philadelphia, Pennsylvania 19112	1
Mr. A. M. Anzalone Administrative Librarian PLASTEC/ARRADCOM Bldg 3401 Dover, New Jersey 07801	1

DL/413/83/01
359/413-2

TECHNICAL REPORT DISTRIBUTION LIST, 359

Dr. Paul Delahay
Department of Chemistry
New York University
New York, New York 10003

Dr. P. J. Hendra
Department of Chemistry
University of Southampton
Southampton SO9 5NH
United Kingdom

Dr. T. Katan
Lockheed Missiles and
Space Co., Inc.
P.O. Box 504
Sunnyvale, California 94088

Dr. D. N. Bennion
Department of Chemical Engineering
Brighma Young University
Provo, Utah 84602

Dr. R. A. Marcus
Department of Chemistry
California Institute of Technology
Pasadena, California 91125

Mr. Joseph McCartney
Code 7121
Naval Ocean Systems Center
San Diego, California 92152

Dr. J. J. Auborn
Bell Laboratories
Murray Hill, New Jersey 07974

Dr. Joseph Singer, Code 302-1
NASA-Lewis
21000 Brookpark Road
Cleveland, Ohio 44135

Dr. P. P. Schmidt
Department of Chemistry
Oakland University
Rochester, Michigan 48063

Dr. H. Richtol
Chemistry Department
Rensselaer Polytechnic Institute
Troy, New York 12181

Dr. E. Yeager
Department of Chemistry
Case Western Reserve University
Cleveland, Ohio 44106

Dr. C. E. Mueller
The Electrochemistry Branch
Naval Surface Weapons Center
White Oak Laboratory
Silver Spring, Maryland 20910

Dr. Sam Perone
Chemistry & Materials
Science Department
Lawrence Livermore National Lab.
Livermore, California 94550

Dr. Royce W. Murray
Department of Chemistry
University of North Carolina
Chapel Hill, North Carolina 27514

Dr. G. Goodman
Johnson Controls
5757 North Green Bay Avenue
Milwaukee, Wisconsin 53201

Dr. B. Brummer
EIC Incorporated
111 Chapel Street
Newton, Massachusetts 02158

Dr. Adam Heller
Bell Laboratories
Murray Hill, New Jersey 07974

Electrochimica Corporation
Attn: Technical Library
2485 Charleston Road
Mountain View, California 94040

Library
Duracell, Inc.
Burlington, Massachusetts 01803

Dr. A. B. Ellis
Chemistry Department
University of Wisconsin
Madison, Wisconsin 53706

DL/413/83/01
359/413-2

TECHNICAL REPORT DISTRIBUTION LIST, 359

Dr. M. Wrighton
Chemistry Department
Massachusetts Institute
of Technology
Cambridge, Massachusetts 02139

Dr. B. Stanley Pons
Department of Chemistry
University of Utah
Salt Lake City, Utah 84112

Donald E. Mains
Naval Weapons Support Center
Electrochemical Power Sources Division
Crane, Indiana 47522

S. Ruby
DOE (STOR)
M.S. 6B025 Forrestal Bldg.
Washington, D.C. 20595

Dr. A. J. Bard
Department of Chemistry
University of Texas
Austin, Texas 78712

Dr. Janet Osteryoung
Department of Chemistry
State University of New York
Buffalo, New York 14214

Dr. Donald W. Ernst
Naval Surface Weapons Center
Code R-33
White Oak Laboratory
Silver Spring, Maryland 20910

Mr. James R. Moden
Naval Underwater Systems Center
Code 3632
Newport, Rhode Island 02840

Dr. Bernard Spielvogel
U.S. Army Research Office
P.O. Box 12211
Research Triangle Park, NC 27709

Dr. William Ayers
ECD Inc.
P.O. Box 5357
North Branch, New Jersey 08876

Dr. M. M. Nicholson
Electronics Research Center
Rockwell International
3370 Miraloma Avenue
Anaheim, California

Dr. Michael J. Weaver
Department of Chemistry
Purdue University
West Lafayette, Indiana 47907

Dr. R. David Rauh
EIC Corporation
111 Chapel Street
Newton, Massachusetts 02158

Dr. Aaron Wold
Department of Chemistry
Brown University
Providence, Rhode Island 02192

Dr. Martin Fleischmann
Department of Chemistry
University of Southampton
Southampton SO9 5NH ENGLAND

Dr. R. A. Osteryoung
Department of Chemistry
State University of New York
Buffalo, New York 14214

Dr. Denton Elliott
Air Force Office of Scientific
Research
Bolling AFB
Washington, D.C. 20332

Dr. R. Nowak
Naval Research Laboratory
Code 6130
Washington, D.C. 20375

Dr. D. F. Shriver
Department of Chemistry
Northwestern University
Evanston, Illinois 60201

Dr. Aaron Fletcher
Naval Weapons Center
Code 3852
China Lake, California 93555

DL/413/83/01
359/413-2

TECHNICAL REPORT DISTRIBUTION LIST, 359

Dr. David Aikens
Chemistry Department
Rensselaer Polytechnic Institute
Troy, New York 12181

Dr. A. P. B. Lever
Chemistry Department
York University
Downsview, Ontario M3J1P3

Dr. Stanislaw Szpak
Naval Ocean Systems Center
Code 6343, Bayside
San Diego, California 95152

Dr. Gregory Farrington
Department of Materials Science
and Engineering
University of Pennsylva a
Philadelphia, Pennsylvania 19104

M. L. Robertson
Manager, Electrochemical
and Power Sources Division
Naval Weapons Support Center
Crane, Indiana 47522

Dr. T. Marks
Department of Chemistry
Northwestern University
Evanston, Illinois 60201

Dr. Micha Tomkiewicz
Department of Physics
Brooklyn College
Brooklyn, New York 11210

Dr. Lesser Blum
Department of Physics
University of Puerto Rico
Rio Piedras, Puerto Rico 00931

Dr. Joseph Gordon, II
IBM Corporation
K33/281
5600 Cottle Road
San Jose, California 95193

Dr. D. H. Whitmore
Department of Materials Science
Northwestern University
Evanston, Illinois 60201

Dr. Alan Bewick
Department of Chemistry
The University of Southampton
Southampton, SO9 5NH ENGLAND

Dr. E. Anderson
NAVSEA-56Z33 NC #4
2541 Jefferson Davis Highway
Arlington, Virginia 20362

Dr. Bruce Dunn
Department of Engineering &
Applied Science
University of California
Los Angeles, California 90024

Dr. Elton Cairns
Energy & Environment Division
Lawrence Berkeley Laboratory
University of California
Berkeley, California 94720

Dr. D. Cipris
Allied Corporation
P.O. Box 3000R
Morristown, New Jersey 07960

Dr. M. Philpott
IBM Corporation
5600 Cottle Road
San Jose, California 95193

Dr. Donald Sandstrom
Department of Physics
Washington State University
Pullman, Washington 99164

Dr. Carl Kannewurf
Department of Electrical Engineering
and Computer Science
Northwestern University
Evanston, Illinois 60201

DL/413/83/01
359/413-2

TECHNICAL REPORT DISTRIBUTION LIST, 359

Dr. Robert Somoano
Jet Propulsion Laboratory
California Institute of Technology
Pasadena, California 91103

Dr. Johann A. Joebstl
USA Mobility Equipment R&D Command
DRDME-EC
Fort Belvoir, Virginia 22060

Dr. Judith H. Ambrus
NASA Headquarters
M.S. RTS-6
Washington, D.C. 20546

Dr. Albert R. Landgrebe
U.S. Department of Energy
M.S. 6B025 Forrestal Building
Washington, D.C. 20595

Dr. J. J. Brophy
Department of Physics
University of Utah
Salt Lake City, Utah 84112

Dr. Charles Martin
Department of Chemistry
Texas A&M University
College Station, Texas 77843

Dr. H. Tachikawa
Department of Chemistry
Jackson State University
Jackson, Mississippi 39217

Dr. Theodore Beck
Electrochemical Technology Corp.
3935 Leary Way N.W.
Seattle, Washington 98107

Dr. Farrell Lytle
Boeing Engineering and
Construction Engineers
P.O. Box 3707
Seattle, Washington 98124

Dr. Robert Gotscholl
U.S. Department of Energy
MS G-226
Washington, D.C. 20545

Dr. Edward Fletcher
Department of Mechanical Engineering
University of Minnesota
Minneapolis, Minnesota 55455

Dr. John Fontanella
Department of Physics
U.S. Naval Academy
Annapolis, Maryland 21402

Dr. Martha Greenblatt
Department of Chemistry
Rutgers University
New Brunswick, New Jersey 08903

Dr. John Wasson
Syntheco, Inc.
Rte 6 - Industrial Pike Road
Gastonia, North Carolina 28052

Dr. Walter Roth
Department of Physics
State University of New York
Albany, New York 12222

Dr. Anthony Sammells
Eltron Research Inc.
710 E. Ogden Avenue #108
Naperville, Illinois 60540

Dr. W. M. Risen
Department of Chemistry
Brown University
Providence, Rhode Island 02192

Dr. C. A. Angell
Department of Chemistry
Purdue University
West Lafayette, Indiana 47907

Dr. Thomas Davis
Polymer Science and Standards
Division
National Bureau of Standards
Washington, D.C. 20234


DAT
FILM